

# Central Pattern Generating Neurons Simultaneously Express Fast and Slow Rhythmic Activities in the Stomatogastric Ganglion

Dirk Bucher, Adam L. Taylor and Eve Marder

*J Neurophysiol* 95:3617-3632, 2006. First published Feb 22, 2006; doi:10.1152/jn.00004.2006

## You might find this additional information useful...

---

This article cites 80 articles, 51 of which you can access free at:

<http://jn.physiology.org/cgi/content/full/95/6/3617#BIBL>

Updated information and services including high-resolution figures, can be found at:

<http://jn.physiology.org/cgi/content/full/95/6/3617>

Additional material and information about *Journal of Neurophysiology* can be found at:

<http://www.the-aps.org/publications/jn>

---

This information is current as of May 10, 2007 .

# Central Pattern Generating Neurons Simultaneously Express Fast and Slow Rhythmic Activities in the Stomatogastric Ganglion

Dirk Bucher, Adam L. Taylor, and Eve Marder

*Volen Center and Biology Department, Brandeis University, Waltham, Massachusetts*

Submitted 3 January 2006; accepted in final form 21 February 2006

**Bucher, Dirk, Adam L. Taylor, and Eve Marder.** Central pattern generating neurons simultaneously express fast and slow rhythmic activities in the stomatogastric ganglion. *J Neurophysiol* 95: 3617–3632, 2006. First published February 22, 2006; doi:10.1152/jn.00004.2006. Neuronal firing patterns can contain different temporal information. It has long been known that the fast pyloric and the slower gastric motor patterns in the stomatogastric ganglion of decapod crustaceans interact. However, the bidirectional influences between the pyloric rhythm and the gastric mill rhythm have not been quantified in detail from preparations that spontaneously express both patterns *in vitro*. We found regular and stable spontaneous gastric and pyloric activity in 71% of preparations of the isolated stomatogastric nervous system of the lobster, *Homarus americanus*. The gastric [cycle period:  $10.96 \pm 2.67$  (SD) s] and pyloric (cycle period:  $1.35 \pm 0.18$  s) patterns showed bidirectional interactions and coordination. Gastric neuron firing showed preferred phases within the reference frame of the pyloric cycle. The relative timing and burst parameters of the pyloric neurons systematically changed within the reference frame of the gastric cycle. The gastric rhythm showed a tendency to run at cycle periods that were integer multiples of the pyloric periods, but coupling and coordination between the two rhythms were variable. We used power spectra to quantify the gastric and pyloric contributions to the firing pattern of each individual neuron. This provided us with a way to analyze the firing pattern of each gastric and pyloric neuron type individually without reference to either gastric or pyloric phase. Possible functional consequences of these network interactions for motor output are discussed.

## INTRODUCTION

Neurons and networks can produce activity that simultaneously carries information about different processes. This is achieved either by coding different information in different frequency bands or by using different coding modalities at different time scales. For example, network oscillations in the mammalian forebrain at different frequency bands can either be associated with different brain states, or coexist and interact (Buzsaki and Chrobak 1995; Buzsaki and Draguhn 2004; Steriade 2005). In the zebrafish olfactory bulb, seemingly alternative coding strategies, namely rate coding and spike synchrony, potentially coexist (Friedrich et al. 2004). Electrosensory pyramidal cells in weakly electric fish produce spike trains in response to broadband input that consist of two parallel information streams, one using bursts and one using single spikes (Oswald et al. 2004).

Examples of simultaneous expression of more than one pattern are also found in neuronal and network activity that

produces different rhythmic motor output at different cycle periods. Interactions between either motor patterns can be due to sensory feedback that reports movement of one part of the body and affects pattern generation for another part or to central connections between central pattern generating (CPG) circuits (Marder et al. 2005). For example, the respiratory CPG in the rat can be reset and entrained at integer multiples of the period of rhythmic sensory feedback reporting leg movements. This is thought to provide coordination between locomotion and breathing (Morin and Viala 2002; Potts et al. 2005).

In contrast, interactions between networks in the stomatogastric nervous system (STNS) are present even in the absence of sensory feedback. The STNS controls rhythmic movements in different parts of the stomach in decapod crustaceans (Harris-Warrick et al. 1992; Selverston and Moulins 1987). The stomatogastric ganglion (STG) contains two networks, one controlling the teeth of the gastric mill and one controlling the pyloric filter apparatus. These networks are composed of neurons that act both as part of their respective CPGs and as motor neurons that send axons to specific stomach muscles. The gastric pattern has a cycle period on the order of 5–20 s, whereas the pyloric pattern has a cycle period on the order of 1–2 s.

STG neurons, as well as other neurons in the STNS, can switch from one pattern to another, and modulatory input can reconfigure circuits to produce different types of coordination between neurons controlling separate parts of the stomach (Dickinson 1995; Dickinson et al. 1990; Hooper and Moulins 1989, 1990; Marder et al. 2005; Meyrand et al. 1991, 1994; Weimann and Marder 1994). Many of these neurons also express rhythmic activity of multiple patterns at the same time, reflecting influences of two or more networks. Gastric neurons can show clear pyloric modulation of their firing pattern during the phase in the gastric cycle in which they are active, and pyloric neurons can show modulation of their bursting activity over the course of a gastric cycle (Heinzel 1988a; Heinzel and Selverston 1988; Mulloney 1977; Thuma and Hooper 2002; Weimann et al. 1991). These interactions are mediated by direct chemical and electrical synapses between members of the pyloric and gastric networks (Bartos et al. 1999; Clemens et al. 1998; Mulloney 1977; Selverston et al. 1976) and by coordinating influences from descending neurons (Bartos and Nusbaum 1997; Wood et al. 2004).

Coordinated activity among two or more CPGs is important for behavior involving multiple body parts. However, the presence of interactions between two CPGs does not automat-

Present address and address for reprint requests and other correspondence: D. Bucher, Whitney Laboratory and Department of Neuroscience, University of Florida, 9505 Ocean Shore Blvd., St. Augustine, FL 32080 (E-mail: bucher@whitney.ufl.edu).

The costs of publication of this article were defrayed in part by the payment of page charges. The article must therefore be hereby marked "advertisement" in accordance with 18 U.S.C. Section 1734 solely to indicate this fact.

ically mean that there is coordination between the motor patterns. Nadim et al. (1998) and Bartos et al. (1999) have shown that there is integer locking between the gastric and pyloric cycle periods in a specific version of activity elicited by a single projection neuron, MCN1, in *Cancer borealis*. In contrast, spontaneous gastric and pyloric activity in *Panulirus interruptus* does not show integer locking (Thuma and Hooper 2002). In the latter case, analyzing the dynamics of one pattern within the reference frame of the other is problematic because averaging between cycles leads to underestimation of the magnitude of the effects.

Here for the first time, we provide quantitative analyses of the interactions between spontaneous pyloric and gastric activity. We do so in three different ways. First, we used the isolated STNS of *Homarus americanus* to analyze gastric neuron firing within the reference frame of the pyloric cycle. Second, we analyzed pyloric neuron firing within the reference frame of the gastric cycle. Third, we analyzed the firing patterns of each neuron type individually with respect to how much each rhythm contributes to the firing patterns. Together these data provide a baseline quantitative description of network interactions in the *H. americanus* STG. Such a description will be useful for understanding how neuromodulatory inputs might alter the extent to which networks interact and how the discharge patterns of individual neurons reflect these interactions.

## METHODS

Adult lobsters, *H. americanus* (weight: ~500 g), were purchased from Yankee Lobster (Boston, MA). Animals were kept at 10–13°C in recirculating artificial seawater tanks. All animals were cold-anesthetized prior to dissection. Dissections were carried out in saline containing (in mM) 479.12 NaCl, 12.74 KCl, 13.67 CaCl<sub>2</sub>, 20 MgSO<sub>4</sub>, 3.91 Na<sub>2</sub>SO<sub>4</sub>, and 5 HEPES, pH = 7.4–7.5. The STNS was dissected and pinned out in transparent silicone elastomer (Sylgard)-coated (Dow Corning, Midland, MI) dishes containing chilled (9–13°C) saline. The paired commissural ganglia (CoGs), the esophageal ganglion (OG), the STG, their connecting nerves, and many of the peripheral motor nerves were kept intact. The STG was always desheathed.

### Electrophysiological recordings

Maynard and Dando (1974) described the innervation of the stomach muscles in *H. americanus* using slightly different terminology than the one Mulloney and Selverston (1974) established for the spiny lobster, *P. interruptus*. Because the latter has prevailed in a number of different species, including the closely related *Homarus gammarus* (e.g., Robertson and Moulins 1984), we also adopted it for *H. americanus*.

Figure 1 schematically depicts the innervation pattern of the stomach muscles (Claiborne and Ayers 1987; Maynard and Dando 1974). The lateral gastric (LG) neuron, the dorsal gastric (DG) neuron, the medial gastric (MG) neuron, the gastric mill (GM) neurons, and the lateral posterior gastric (LPG) neurons innervate muscles that move the teeth of the gastric mill. The LPG neurons also innervate pyloric muscles. The GM neurons are responsible for the power stroke of the medial tooth, whereas the LG and MG neurons control the power stroke of the lateral teeth. The DG neuron controls the return stroke of the medial tooth, and the LPG neurons the return stroke of the lateral teeth. The pyloric dilator (PD) neurons and the lateral pyloric (LP) neuron innervate muscles that move the pylorus and the cardio-pyloric valve. The pyloric (PY) neurons innervate muscles that move the pylorus. The ventricular dilator (VD) neuron and the inferior cardiac

(IC) neuron innervate muscles that move the ventral cardiac ossicles, and thereby the cardio-pyloric valve. The anterior median (AM) neuron innervates dorsal cardiac muscles.

Extracellular recordings were obtained by placing stainless steel wires into small (~1 mm) petroleum-jelly wells around specific nerves (Fig. 1B). Signals were amplified and filtered using differential AC amplifiers (A-M Systems, Carlsborg, WA).

Intracellular recordings from the STG neuron somata were made using 20–40 MΩ glass microelectrodes filled with 0.6 M K<sub>2</sub>SO<sub>4</sub> and 20 mM KCl and amplified using an Axoclamp 2B amplifier (Axon Instruments, Foster City, CA). Cells were identified by their characteristic waveforms and correspondence of intracellular spikes with extracellular spikes in the nerve recordings. The pyloric and gastric networks include two interneurons, the anterior burster (AB) and interneuron 1 (Int1). These two neurons have ascending axons in the stomatogastric nerve, but the signal-to-noise ratio in extracellular recordings was low, and we therefore did not include these cells in any quantitative analyses.

### Data acquisition and analysis

Recordings were digitized using a DigiData 1200 data-acquisition board (Axon Instruments) and analyzed with Spike2 (version 5, CED, Cambridge, UK) and MATLAB (version 7, The MathWorks, Natick, MA) using programs written in the respective script languages. Spike time detection was achieved either by using simple thresholding or, if more than one signal amplitude was present in a nerve recording, by using window discrimination. For neurons that exist in two copies (PD and LPG), unambiguous spike detection was still possible because summation of extracellular signals took place only occasionally and could easily be taken into account. However, there are multiple copies of PY and GM neurons, and in the STG of *H. americanus* there is variability in their numbers from animal to animal (Bucher and Marder, unpublished results). The extent of summation of extracellularly recorded signals made unambiguous spike detection impossible for these two neuron types. Therefore wherever changes in number of spikes and spike frequency are described for the PY and GM neurons here, they represent relative rather than exact measures.

Statistical tests and plots were performed in MATLAB and Statview (version 5, SAS Institute, Cary, NC). Figures were done in Canvas (version 10, ADC Systems, Miami, FL). Error bars represent SD to indicate the variability of a sample and SE when statistical comparisons were performed. Data presented here are from a total of 45 animals in which different combinations of extra- and intracellular recordings were obtained. Unless indicated otherwise, for comparisons across different neurons only experiments were analyzed in which recordings of all of these neurons were present. For all statistical analyses, 10–20 min of continuous recordings were used.

### Spectral analysis

Power spectra were used to estimate how much of the variability in a neuron's spike rate was at pyloric/gastric frequencies. Our approach was similar to that of Miller and Sigvardt (1998) but with a few differences. All spectra were estimated from extracellular recordings of a given neuron's spike train that were 1,200 s in duration. Extracellular recordings were converted to spike times using a simple threshold-crossing method. Spikes that occurred within 20 ms of other spikes were deleted, to eliminate spuriously high instantaneous spike rates (this occurs, for instance, in the PD recordings because the 2 PDs sometimes fire nearly simultaneously). Each spike train was converted into a spike rate,  $r(t)$ , defined as one over the interspike interval of the spikes just before and after a given time  $t$ . The "sampling rate" for  $r(t)$  was 1 kHz. Power spectra were estimated from the  $r(t)$  signal using multitaper spectral estimation (Percival and Walden 1993). Each 1,200-s-long signal was divided into 12 100-s-long windows, and a spectrum was estimated for each, using a single taper. The mean of



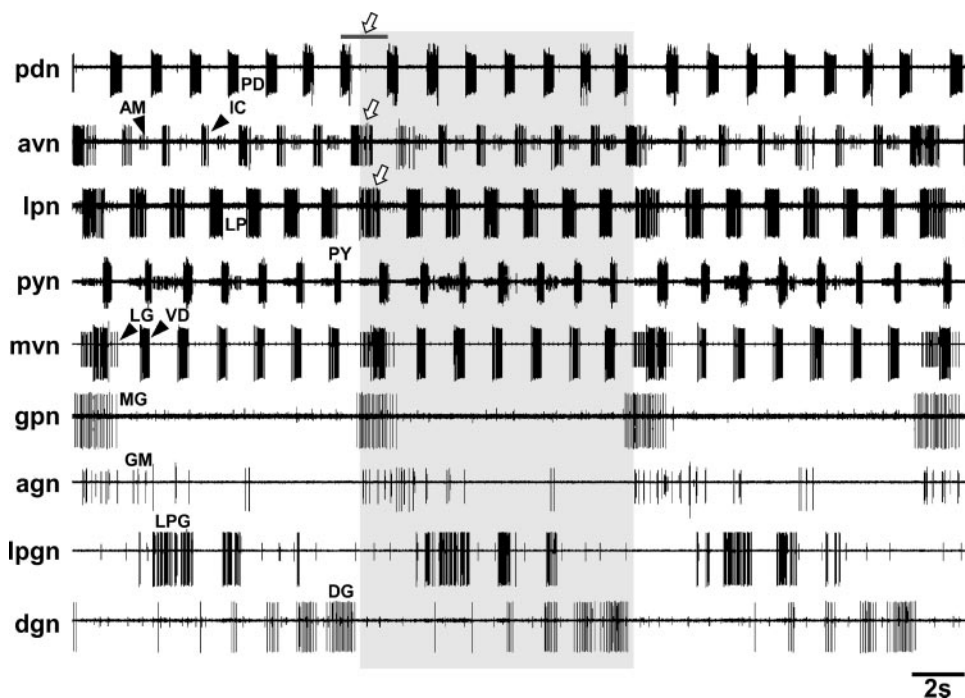


FIG. 2. Simultaneous extracellular nerve recordings of all STG motor neurons. One cycle of the gastric mill rhythm (between 2 LG burst starts) is indicated by gray shading. Note the strong pyloric modulation of the DG neuron and LPG neuron firing patterns. Gastric effects on pyloric neuron firing pattern can also be seen: open arrows indicate longer pyloric period (between 2 PD burst starts) and longer IC and LP burst durations near the start of the gastric cycle.

we observed, we found that it was possible to consistently label each cell as either “gastric” or “pyloric.” We called a neuron pyloric if it showed continuous pyloric bursting activity throughout the entire gastric cycle. We called a neuron gastric if it was only active in specific phases of the gastric cycle, regardless of how much pyloric timing it expressed in its firing pattern. We found that each identified neuron received the same classification in all preparations that expressed both gastric and pyloric activity.

The cells classified as pyloric by the preceding rule were the PD, LP, PY, VD, IC, and AM neurons. The AM neuron was either silent or firing in pyloric time. The AM neuron also fires in pyloric time in *H. gammarus* (Nagy et al. 1994), whereas it is predominantly active in gastric time in *C. borealis* and *P. interruptus* (Selverston et al. 1976; Weimann et al. 1991). The VD and IC neurons were never silent in part of the gastric cycle as they can be in *C. borealis* (Weimann et al. 1991, 1993), and *P. interruptus* (Mulloney 1977; Thuma and Hooper 2002).

The cells classified as gastric by the preceding rule include all neurons that innervate muscles that move the teeth of the gastric mill (LG, DG, MG, and GM neurons), and the LPG neurons, which innervate both gastric and pyloric muscles.

#### Gastric and pyloric rhythm cycle periods

We used either the PD neuron or the VD neuron burst starts to measure the mean pyloric cycle period in all preparations, and, if present, the LG neuron burst starts to measure the mean gastric cycle period. In *C. borealis*, the periods of gastric and pyloric rhythms are strongly correlated when both rhythms are elicited through stimulation of the projection neuron MCN1 (Bartos et al. 1999; Nadim et al. 1998). In *H. americanus*, we found that the pyloric rhythm period was significantly longer in preparations that did not express a gastric rhythm ( $1.78 \pm 0.41$  s,  $n = 10$ ), than in preparations that did ( $1.35 \pm 0.18$  s,  $n = 32$ ) (unpaired *t*-test,  $P < 0.0001$ , Fig. 3A). However, in

preparations with both rhythms present (gastric period =  $10.96 \pm 2.67$  s), the gastric cycle period and the pyloric cycle period were not correlated (linear regression,  $R^2 = 0.03$ ,  $P = 0.32$ , Fig. 3B).

#### Phase relationships of the gastric rhythm

We analyzed the gastric rhythm within the reference frame of its own cycle. The phase relationships of the gastric neurons have not previously been quantified in *H. americanus*. Because of the complex patterns of spike timing within the bursts of gastric neurons, we felt that plotting the phase relationships as the commonly used bar charts would fail to represent a salient feature of the temporal dynamics of spiking activity in the gastric cycle, namely the changing spike rate during the burst. In addition, for some of the neurons, strong pyloric modulation of their firing pattern made unambiguous detection of burst starts and burst ends difficult. We therefore divided the gastric cycle into bins and plotted histograms of the normalized

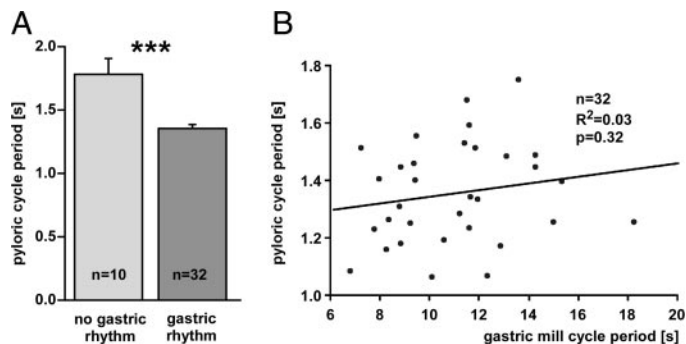


FIG. 3. Gastric and pyloric cycle periods. A: pyloric rhythm period is longer in preparations in which no gastric rhythm was present (unpaired *t*-test,  $P < 0.0001$ ). B: in preparations with gastric activity, the gastric and pyloric cycle periods are not correlated ( $n = 32$ , regression analysis:  $R^2 = 0.03$ ,  $P = 0.32$ ).

number of spikes per bin (spike density) similar to the method used in Faumont et al. (1998).

The phase histograms shown in Fig. 4 were generated in the following way: LG neuron burst starts were chosen as the reference point because they were the most regular and consistent feature in the gastric cycle. For each experiment, the time between two consecutive LG neuron burst starts was divided into 100 bins and, for each cycle and for every neuron, all spikes were sorted into the corresponding bin. The spike count per bin was then divided by the total number of spikes in that experiment and multiplied by 100, so that each bin value represents the percentage of spikes that fell into that bin (i.e., every bin value would be 1 if a neuron showed no preferred firing phase). Figure 4A shows superimposed line plots of the histograms from 10 experiments. Three cycles are shown to give a better sense of the repetitive pattern.

The phase relationships were generally consistent from animal to animal. The “power stroke neurons,” LG, MG, and GM, generally fired in the same phase. In some experiments, the MG neuron and the GM neurons show small peaks corresponding to pyloric modulation during their burst phase as well as small peaks outside of that phase, which correspond to “trailing” pyloric firing (down arrows). The “return stroke neurons”, DG and LPG, fired in anti-phase to the LG, MG, and GM neurons but with different spike profiles during their respective bursts. The DG neuron shows increasing spike density during the burst, and the LPG neuron shows decreasing spike density during the burst. In some experiments, both show small peaks during that phase, which correspond to substantial pyloric modulation of their firing rate (down arrows). DG neuron activity in its specific gastric phase consisted mostly of pyloric-timed bursts of increasing strength, whereas LPG neuron activity consisted mostly of pyloric-timed bursts of decreasing strength.

Figure 4B shows histograms of the mean bin values between experiments (shaded areas, SD). Here, each bin in each histogram represents the mean percentage of spikes that fell into that bin. The mean phase relationships and spike dynamics basically are the same as the ones described for the single experiments. However, pyloric modulation of the spike patterns is less apparent. This is due to the fact that the number of pyloric cycles per gastric cycle can differ substantially from experiment to experiment (see following text). Therefore peaks from pyloric influences are averaged out between experiments.

We found similar phase relationships and spike dynamics within the bursts in all experiments analyzed. On a qualitative level, the same was true for recordings of incomplete sets of gastric neurons which we did not include in our analysis. Only the LPG neurons’ onset phase was quite variable between experiments, but no distinct types of phase relationships were apparent.

#### *Pyloric modulation of gastric neurons*

Gastric neurons are modulated in pyloric time. This is apparent both in the spike rates and in their membrane potential measured with intracellular recordings. Figure 5 shows example intracellular recordings of all gastric neurons (including the interneuron Int1, which was not part of our analysis from extracellular recordings). In the LG, MG, and GM neurons, the pyloric-timed modulation is particularly apparent between strong gastric-timed bursts, whereas Int1 and the DG and LPG

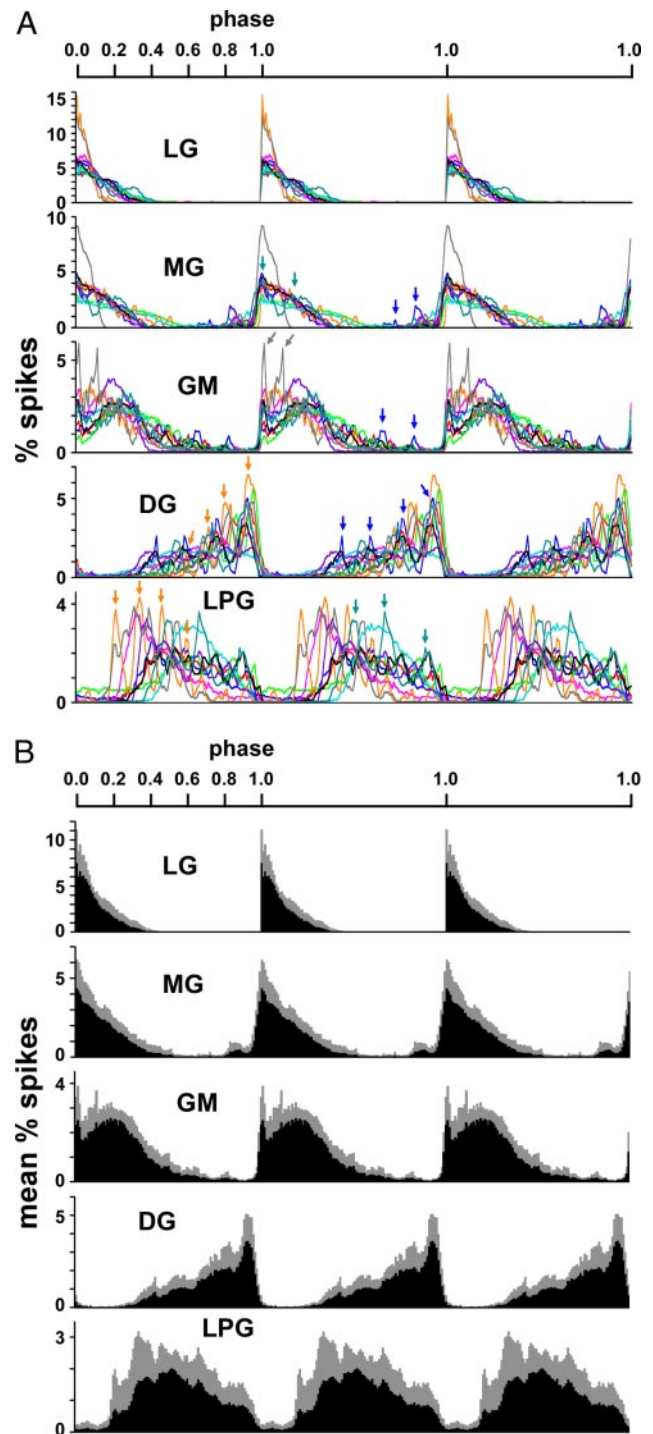


FIG. 4. Phase relationships of gastric neurons. *A*: phase histograms of spike densities from 10 different experiments. The gastric period (between consecutive LG neuron burst starts) was divided into 100 bins, and for every cycle, spikes were sorted into corresponding bins. Bin values were then divided by the total number of spikes. In some experiments, the MG and GM neurons display peaks that correspond to pyloric modulation during their burst phase as well as peaks corresponding to trailing pyloric-timed spiking between bursts ( $\downarrow$ ). The DG and LPG neurons display pyloric-timed modulation during the peaks ( $\downarrow$ ). *B*: phase histograms of the mean normalized spike densities from all 10 experiments.  $\square$ , SD. Due to averaging, the pyloric-timed modulation is less apparent than in the histograms from single experiments.

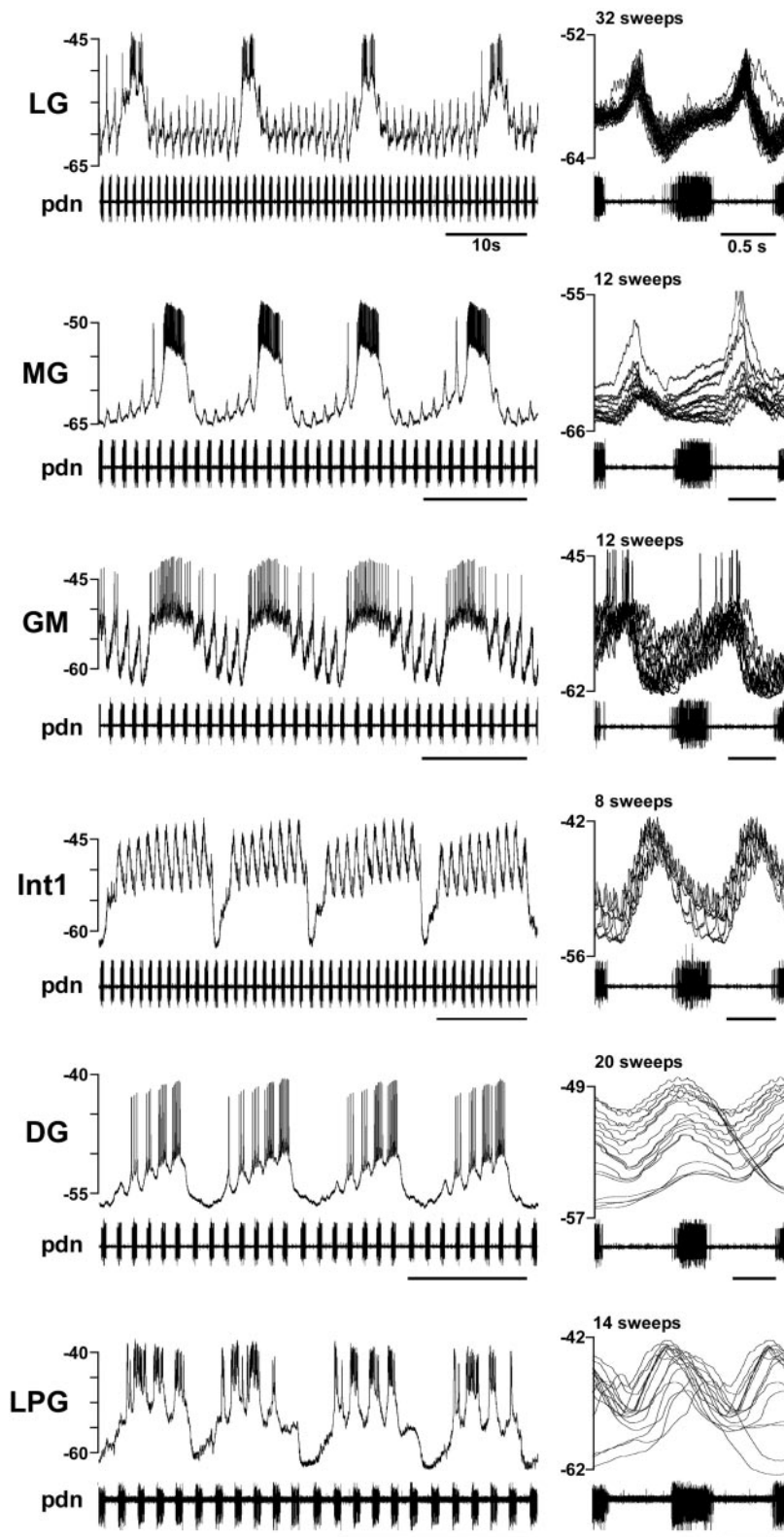


FIG. 5. Pyloric modulation of gastric neuron membrane potential (mV). The LG, MG, and GM neurons show strong pyloric-timed modulation during their interburst intervals, whereas Int1 and the DG and LPG neurons display strong pyloric-timed modulation during their bursts. *Right*: multiple sweeps triggered from selected PD neuron burst starts to show the membrane potential modulation in the pyloric phase. For the LG, MG, and GM neurons, only cycles during the interburst intervals were used. For Int1 and the DG and LPG neurons, only cycles during the burst were used. For clarity, spikes in the DG and LPG neurons were eliminated by low-pass filtering.

neurons show clear pyloric-timed modulation during their gastric-timed bursts. Figure 5, *right*, shows multiple sweeps of the recordings, each triggered by the extracellularly recorded PD neuron burst starts in selected cycles. For the LG, MG, and GM neurons, only pyloric cycles between strong gastric bursts are shown. For the DG and LPG neurons and Int1, only pyloric

cycles during the gastric bursts are shown. For clarity, the DG and LPG neuron recordings were low-pass filtered to mask spikes. We inspected the pyloric-timed membrane potential oscillations in gastric neurons in at least five experiments per neuron type. During their interburst interval, the LG, MG, and GM neurons were consistently hyperpolarized during PD neu-

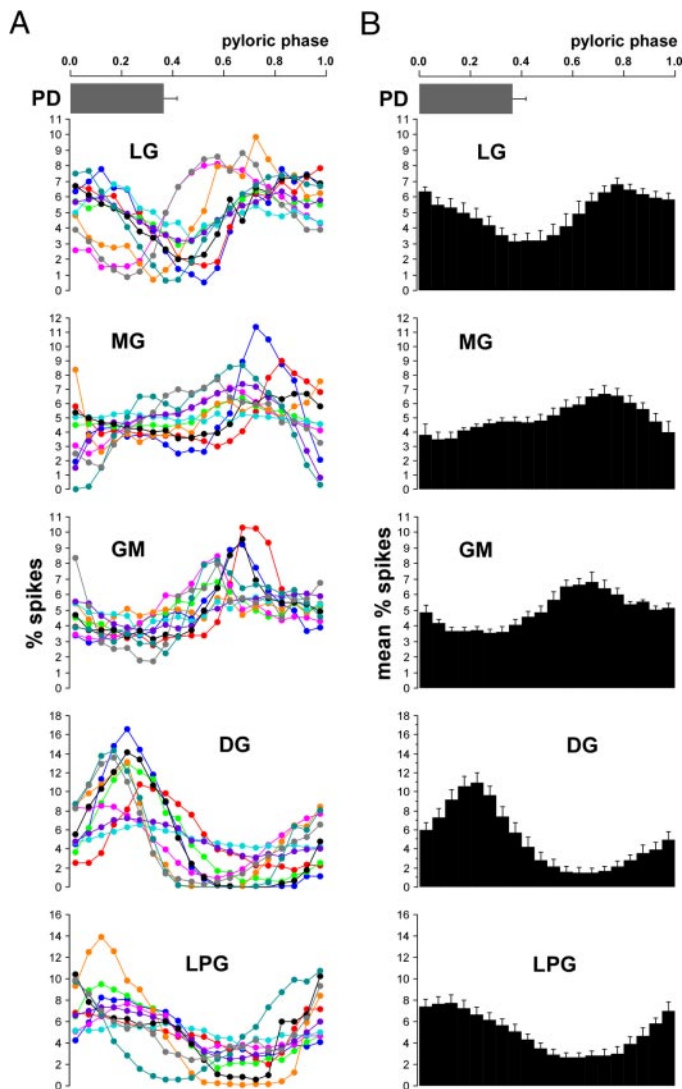


FIG. 6. Pyloric modulation of gastric neuron spike rate. *A*: line plots of histograms from 10 experiments. The pyloric phase was divided into 20 bins, and gastric neuron spikes were sorted in to the corresponding bins. Bin values were normalized to show percentage of counts per bin. The PD duty cycle (+SD) is indicated on top. *B*: bar plots of histograms of the mean normalized counts for all 10 experiments. Error bars are SEs. All measures show different percentages of spikes in different phases of the PD cycle (repeated-measures ANOVA,  $P < 0.0001$  for all measures).

ron bursts. During its bursts, Int1 was consistently hyperpolarized while the PD neuron was firing. During DG neuron bursts, PD neuron bursts coincided with membrane potential depolarizations, and during LPG bursts, PD neuron bursts coincided with the transition from depolarized to hyperpolarized membrane potentials. It should be noted that the conduction delay between the STG and the pdn in *H. americanus* is only 30–50 ms (Bucher et al. 2003, 2005), thus introducing an error of maximally 5% into our measurements of relative timing between gastric neurons and PD neurons.

Pyloric modulation of gastric neurons is also evident in their spike rates. We quantified this from extracellular recordings in the following way: in 10 experiments, the pyloric cycle (between 2 consecutive PD burst starts) was divided into 20 bins, and every gastric neuron spike was sorted into the corresponding bin. Then, every bin count was divided by the total number

of spikes and multiplied by 100 so that every bin value represents the percentage of spikes at the corresponding pyloric phase.

Figure 6*A* shows line plots of the histograms for each experiment and each gastric cell type. Despite some variability between animals, spike densities peaked at roughly the same phases between experiments. Figure 6*B* shows bar plots of the mean bin values from all experiments (+SE). All five cell types show different percentages of spikes in different phases of the PD cycle (repeated-measures ANOVA,  $P < 0.0001$  for all measures). LG, MG, and GM firing peaked during the interburst phase of the PD neurons, whereas DG and LPG firing peaked during the PD neuron burst phase.

#### Phase relationships of the pyloric rhythm

The phase relationships of the PD, LP, and PY neurons have been described in detail before in *H. americanus* (Bucher et al. 2005; Thirumalai and Marder 2002) and *H. gammarus* (Meyr and et al. 2000), but the VD neuron and the IC neuron were not previously included in any quantitative studies. Figure 7 shows a bar chart of the pyloric phase relationships. For this analysis, the latency between PD neuron burst starts and the burst starts and ends of all pyloric neurons were measured and divided by the cycle period (i.e., the time between 2 consecutive PD neuron burst starts). Three cycles are shown. Except for the AM neuron (see following text), only recordings were used in which signals of all pyloric neurons were present ( $n = 17$ ; AM:  $n = 7$ ).

The pyloric rhythm is usually described as a triphasic pattern in which the bursts of the pacemaker group, the AB neuron and the electrically coupled PD neurons, are followed by the LP neuron and then the PY neurons. In *C. borealis* and *P. interruptus*, the VD neuron usually fires in the PY neuron phase, and the IC neuron fires in the LP neuron phase (Mulloney 1987; Selverston and Miller 1980; Weimann et al. 1993). In *H. americanus*, the IC neuron bursts between the PD neuron and LP neuron phase, thereby making the pattern appear to have four distinct phases (Fig. 7). Qualitatively, these phase relationships were consistent from animal to animal and not obviously dependent on the cycle period. However, to show statistically significant phase constancy between animals would require a much larger sample, as shown in Bucher et al. (2005), who used data from 99 animals.

The AM neuron was either silent or fired with the VD and PY neurons, sometimes with only one spike per pyloric cycle. We only included robustly bursting AM neurons in our anal-

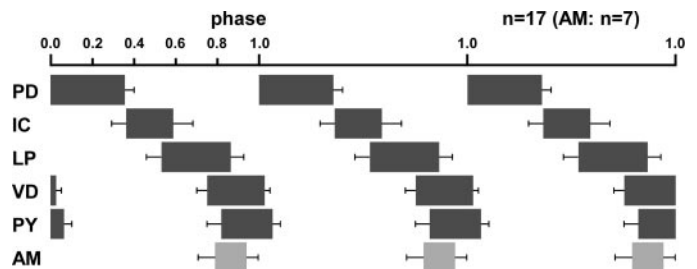


FIG. 7. Phase relationships in the pyloric rhythm ( $n = 17$ ). Three cycles are shown. Note that there appear to be 4 distinct phases: 1) PD, 2) IC, 3) LP, and 4) VD, PY, and AM. Bars indicating the AM neuron burst timing are shaded in lighter gray because this neuron was bursting in only 7 of the 17 preparations. Error bars are SDs.

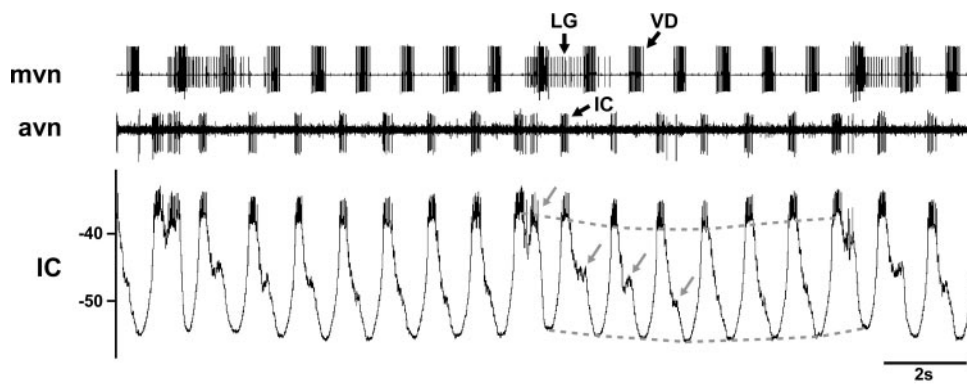


FIG. 8. Gastric modulation of pyloric neuron membrane potential. *Top 2 traces*: extracellular recordings of the LG, VD, and IC neurons. The lower trace shows an intracellular recording of the IC neuron. The pyloric-timed membrane potential oscillations change over the course of the gastric cycle. Arrows indicate the 2nd part of a biphasic depolarization that is strongest at the start of the LG neuron burst and then wanes within a few pyloric cycles. Dashed lines indicate the change in the peaks and troughs of the pyloric-timed oscillation, which are both more depolarized at the time of the start of the LG neuron burst and reach minimum voltages around the middle of the gastric cycle.

ysis. Intracellular recordings from silent AM neurons (not shown) revealed clear pyloric modulation of the membrane potential, peaking approximately with PY and VD activity.

#### Gastric modulation of pyloric neurons

All pyloric neurons showed gastric modulation, albeit to varying degrees. Figure 8 depicts a particularly prominent example of such interactions. An intracellular recording from the IC neuron and extracellular recordings of the IC neuron (avn) and the VD and LG neurons (mvn) are shown. The waveform of the IC neuron membrane potential oscillation, as well as the IC neuron firing pattern, showed clear changes during the gastric period. At the start of the gastric cycle (using the LG neuron as the reference signal), the IC neuron showed a double burst riding on top of a double depolarization that waned over the next few cycles (arrows). In addition, both the peaks and the troughs of the waveform oscillation were at lower membrane potentials in the middle of the gastric cycle (as indicated by broken lines).

We quantified the effect of gastric phase on the firing rate of pyloric neurons (excluding AM) in 12 experiments, using extracellular recordings. We divided the gastric phase (i.e., the time between 2 consecutive LG neuron burst starts) into 10 bins and used the PD neuron burst starts to determine the gastric phase bin in which a particular pyloric cycle took place. We then measured the pyloric cycle period, the number of spikes per burst, and the spike frequencies within bursts for the PD, LP, PY, VD, and IC neurons. We also measured the latency from PD neuron burst start to PD neuron burst end, and the latencies from PD neuron burst starts to burst starts and

ends of the LP, PY, VD, and IC neurons. We calculated the phase relationships of the pyloric rhythm by normalizing the latencies to the pyloric cycle period. Figure 9 shows two examples of these measures and their changes within the gastric rhythm cycle for all 12 experiments. In addition, the mean duty cycle of the LG neuron burst (+SD) is shown. Figure 9A shows the pyloric cycle period and Fig. 9B shows the latency of the PY neuron burst start (with respect to the PD neuron burst start) as a function of the gastric phase. In both cases, all experiments reveal larger values in the two bins around the LG burst start. However, the magnitude of this effect was variable across experiments. Two extreme cases are shown in color for each measure.

Figure 10 shows the mean values of all measures from all experiments. For clarity, SEs are not shown (except for the pyloric cycle period). We tested all measures for significant changes as a function of gastric phase (repeated-measurements ANOVA). The significance level for each measure is indicated by asterisks on the right of the plots. With the exception of the latency of the PD neuron burst end, the phase of the PY neuron burst end, and the PD spike frequency, all measures changed significantly over the gastric cycle. The IC neuron generally shows the largest gastric modulation. Many of the effects, although statistically significant, are small. However, even small changes in the firing pattern may be functionally relevant at their readout, for example the contraction amplitude of pyloric muscles (Morris et al. 2000; Thuma and Hooper 2002; Thuma et al. 2003).

The influence of gastric phase on pyloric rhythm parameters was not consistently strong or weak between different mea-

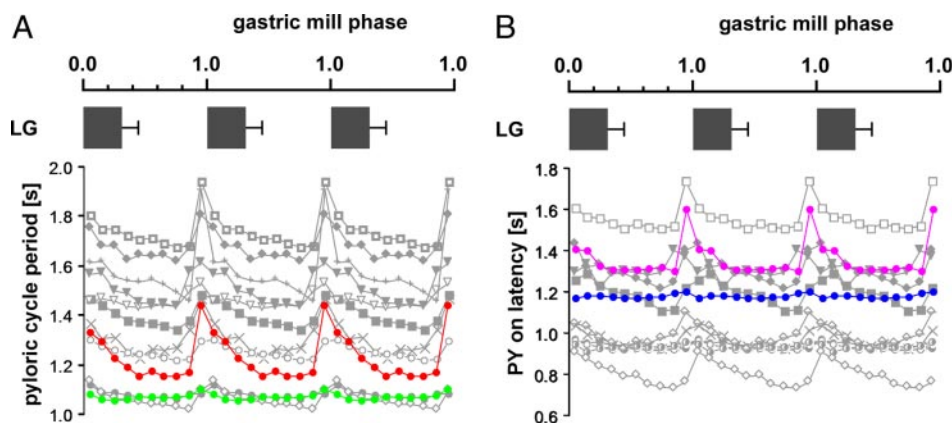
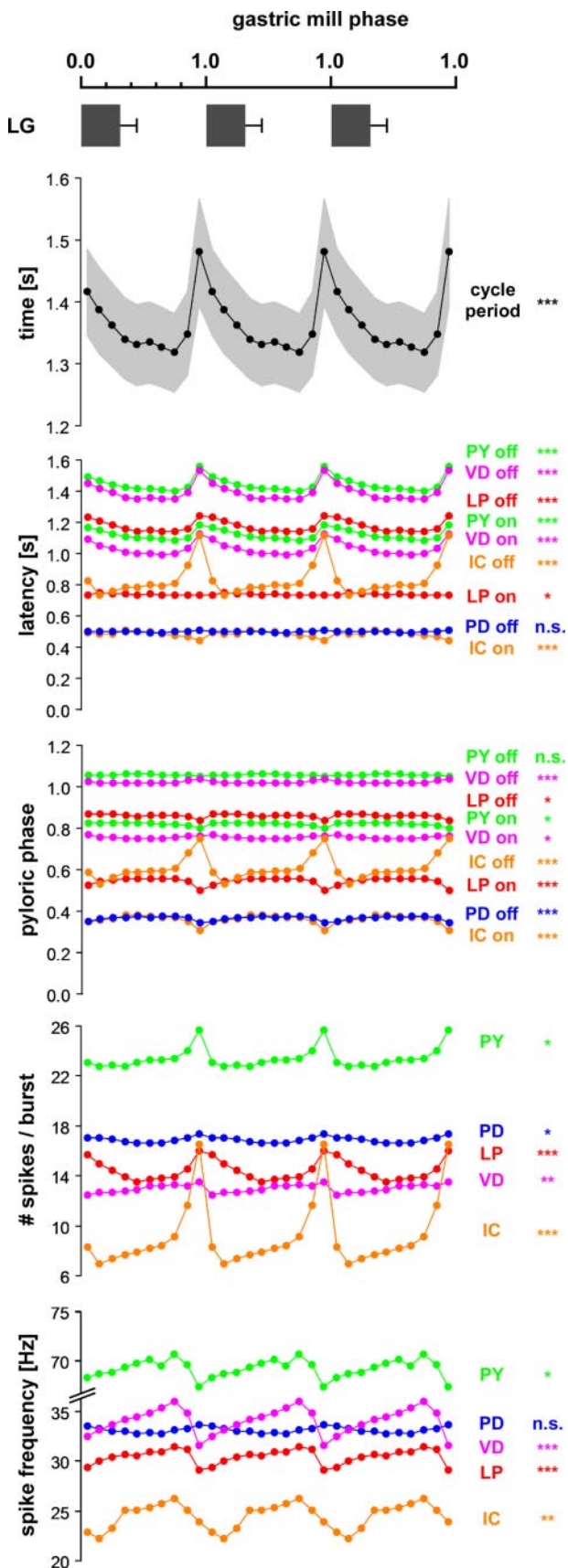


FIG. 9. Gastric modulation of the pyloric rhythm. The gastric phase was divided into 10 bins, and PD neuron burst starts were used to determine the gastric phase in which each pyloric cycle took place. *A*: change of the pyloric cycle period as a function of the gastric phase for 12 experiments. Note that even though peak phases were consistent between experiments, the magnitude of the pyloric cycle period changes was variable. Two extreme cases are shown in color. Gray bars indicate the mean duty cycle of the LG neuron burst (+SD). *B*: same type of plot as in *A*, here for the latency of the PY neuron burst start (with respect to the PD neuron burst start) as a function of the gastric phase. Colored lines in *A* and *B* show data from 4 different experiments.



tures in the same experiment and also did not appear to be correlated with how “strong” the gastric rhythm was. We found no correlation with gastric cycle period, LG burst duration, LG duty cycle, or number of LG spikes per burst (statistical analysis not shown). However, it is possible that a much larger sample size would be needed to establish such correlations.

#### Integer coupling between gastric and pyloric cycle periods

In the preceding analyses, we investigated the dynamics of the firing pattern of gastric neurons and pyloric neurons within the reference frame of the other rhythm and showed that, to some degree, the firing pattern of each STG neuron was affected by the other rhythm. However, the magnitude of effects found with these methods depends not only on the strength of the interaction but also on the extent to which the two rhythms are truly coordinated. Consequently, if the coordination between gastric and pyloric rhythms is not strict, it is problematic to analyze one within the reference frame of the other, because interactions can occur at different phases of the reference cycle (Thuma and Hooper 2002). Therefore we determined the extent to which the gastric cycle periods were integer multiples of the pyloric cycle periods.

To that end, we counted the number of complete pyloric cycles in every gastric cycle, i.e., between two consecutive LG neuron burst starts. For the pyloric cycles occurring around the start and the end of the gastric cycle, we calculated the fractions of their periods that fell into the gastric cycle and added it to the cycle count. This method is illustrated in Fig. 11A. Perfect integer multiple coupling would result in the fraction of the pyloric cycle at the start of the gastric cycle and the fraction at the end adding up to exactly 0 or exactly 1. In contrast, no coupling would result in the sum of the fractions taking any value between 0 and 2. Only experiments in which  $\geq 50$  gastric cycles were recorded were used.

Figure 11B shows histograms from two preparations in which every gastric cycle was scored for the number of pyloric cycles that occurred within it. The pyloric cycle count values were binned (bin size: 0.1), and each bin value was divided by the total number of analyzed gastric cycles in that experiment. Both show peaks around integer numbers in the respective ranges. Figure 11C shows a histogram of the mean fraction of counts of the number of pyloric cycles per gastric cycle for 20 preparations. It shows clear peaks at integer numbers of pyloric cycles.

We also wanted to get a better sense of how consistent this finding was across preparations. We therefore measured the deviation from a given integer value for every gastric cycle in every experiment. With this method, every data point could take any value between  $-0.5$  and  $+0.5$ , meaning that 0 would

FIG. 10. Gastric modulation of the pyloric rhythm. Mean values from 12 experiments. ■, SE for the pyloric cycle period. For clarity, SEs for all other measures are not shown. Significant changes as a function of the gastric cycle are indicated by \* on the left (repeated-measurements ANOVA; n.s.: not significant; \*,  $P < 0.05$ ; \*\*,  $P < 0.01$ ; \*\*\*,  $P < 0.001$ ). Actual  $P$  values: cycle period,  $<0.0001$ ; latency: PD off, 0.2952; LP on, 0.0250; LP off,  $<0.0001$ ; PY on,  $<0.0001$ ; PY off,  $<0.0001$ ; VD on,  $<0.0001$ ; VD off,  $<0.0001$ ; IC on,  $<0.0001$ ; IC off,  $<0.0001$ ; phase: PD off,  $<0.0001$ ; LP on,  $<0.0001$ ; LP off, 0.0350; PY on, 0.0466; PY off, 0.7726; VD on, 0.0432; VD off,  $<0.0001$ ; IC on,  $<0.0001$ ; IC off,  $<0.0001$ ; #spikes/ burst: PD, 0.0290; LP,  $<0.0001$ ; PY, 0.0225; VD, 0.0084; IC,  $<0.0001$ ; spike frequency: PD, 0.3363; LP,  $<0.0001$ ; PY, 0.0467; VD,  $<0.0001$ ; IC, 0.0085.

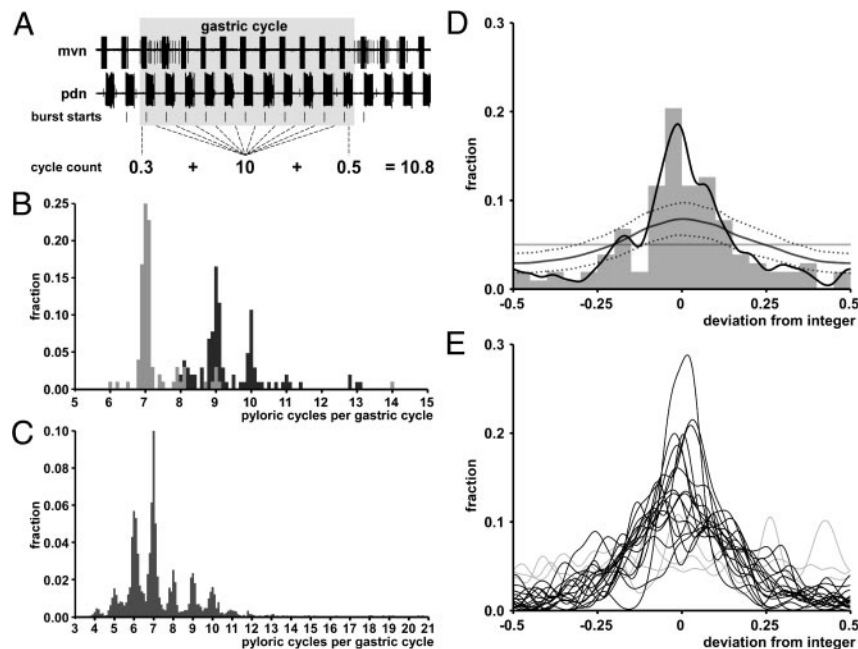


FIG. 11. Integer multiple coupling of pyloric and gastric cycle periods. *A*: recordings of mvn (VD and LG) and pdn (PD). Consecutive LG neuron burst starts were used to define the gastric cycle (■). Pyloric cycles were counted from consecutive burst starts of the PD or VD neuron. The fractions of the pyloric cycles around the start and the end of each gastric cycle were added to the number of complete pyloric cycles within the gastric cycle. *B*: overlaid histograms (bin size = 0.1) of the fraction of the cycle count for 2 experiments. Both peak at integer values in their respected ranges. *C*: histogram of mean normalized cycle counts from 20 experiments. Again, note the peaks at integer values. *D*: deviation from integer values. Histogram (bin size = 0.05) of the deviation from the nearest integer value of pyloric cycles for each gastric cycle in 1 experiment. The black line represents a smoothed distribution generated from a sum of Gaussian functions, each centered on a data point. Values were normalized by dividing by the number of gastric cycles. For comparison, a theoretical flat distribution of the data are shown (straight gray line). The sequence of pyloric cycles was reshuffled to destroy any temporal relationship between the pyloric and gastric rhythms (see text). This was repeated 1,000 times and the deviation from integer measured for each trial. The gray curve and dashed lines are the mean distribution from all trials  $\pm$  SD. The distribution was significantly less concentrated around 0 than the original data ( $P < 0.01$ ). *E*: smoothed histograms from 20 experiments. In 17 experiments, the original data were significantly more concentrated around 0 than the distributions calculated from the reshuffled data.

represent the integer (no matter what the actual integer value for that gastric cycle was), and  $-0.5$  or  $+0.5$  would be the maximum deviation from the integer. A histogram of the integer deviation for each gastric cycle in a single preparation is shown in Fig. 11*D*, along with a smoothed histogram (thick black line). The smoothed histogram was calculated by adding up Gaussian functions at the locations of each of the data points. The SD of these Gaussian functions controlled the degree of smoothing. The smoothed histogram shown in Fig. 11*D* appears to peak near zero deviation, suggesting the presence of integer-coupling.

However, it is possible for such a histogram to have a peak near zero even if there is no true coupling between the two rhythms. This can happen if by mere chance the mean cycle period of one rhythm is an integer multiple of the cycle period of the other, and the cycle-to-cycle variability is small. For instance, consider two clocks. The minute hand of one clock and the second hand of the other clock will appear to be “integer-locked” to the extent they are both faithfully keeping time. But this is not because there is any coupling between them (as would be revealed if you broke one). But the minute hand and the second hand of the *same* clock are integer-locked because even if the cycle period of one varies, the other will track with it.

To distinguish true integer coupling from “incidental” integer coupling, we used a “reshuffling” technique. For each experiment, we first calculated the second moment (the average of the squares of all data points) of the integer deviation data. This should be small for histograms that peak near zero

and larger for ones that do not. We then randomly reshuffled the sequence of pyloric periods to destroy any temporal relationship between the pyloric periods and the gastric period in which they occur. If there was true integer coupling, we would expect the integer deviation histogram to be less concentrated around zero than in the true data. By generating many reshuffled data sets, we can approximate the distribution of second moments for data that contain no true integer coupling. We can then see how much of this reshuffled distribution was more extreme than the value calculated from the data.

The mean of all smoothed histograms from 1,000 reshuffled samples is shown in Fig. 11*D*, along with the mean SD (gray and dashed curves). It is less concentrated around zero than the smoothed histogram from the data, and the SDs suggest that it is significantly so. Indeed we found that the second moment was significantly different from the distribution of second moments for reshuffled data, with  $P < 0.01$ . Overall, we found that 17 of 20 preparations were significantly integer-coupled. A smoothed histogram is shown for each preparation in Fig. 11*E*, with significantly concentrated ones shown in black and not significantly concentrated ones shown in gray.

#### *Firing pattern of individual STG neurons reflects both the pyloric and the gastric rhythm*

In the preceding analysis, we found that coordination between the two rhythms, namely integer multiple coupling, was present to varying degrees. Because this makes analyzing one rhythmic pattern within the reference frame of the other prob-

lematic, we also analyzed the firing pattern of each individual neuron solely based on its spike times.

Figure 12 shows extracellular recordings of the VD, LG, and DG neurons in three different experiments. Figure 12A shows an example in which both the DG and the LG neuron fired strong bursts with many spikes and little apparent modulation in pyloric time. Figure 12B shows an example with weaker firing but strong pyloric modulation of the DG firing pattern. Figure 12C shows an example in which no gastric rhythm was present, the LG neuron was silent, and the DG neuron fired only in pyloric time. In all three examples, the VD neuron showed no apparent modulation of its firing pattern in gastric time.

As a first pass, we used autocorrelation histograms of the spike times to visualize the presence of pyloric and gastric contributions to the firing pattern (Fig. 12, right). The time lag from every spike to every other spike in the same trace, both

forward and backward in time, was plotted as a histogram. With appropriate bin sizes, such plots show peaks at time lags that equal the period and multiples of that period of rhythmic activity. In Fig. 12A, both the LG neuron and the DG neuron show clear peaks at the gastric cycle period with very little, if any, occurrence of smaller peaks corresponding to the pyloric cycle period.

The VD neuron shows clear peaks corresponding to the pyloric cycle period and its multiples. Those peaks have the highest counts at time lags equal to the gastric period (open arrows), as seen in the LG neuron and DG neuron autocorrelations. This is also true for the VD neuron in Fig. 12B, indicating gastric modulation of the VD firing pattern.

In addition to peaks corresponding to the gastric cycle period, the LG neuron and the DG neuron in Fig. 12B show peaks corresponding to the pyloric cycle period. This is barely detectable in the LG neuron but clearly visible in the DG neuron

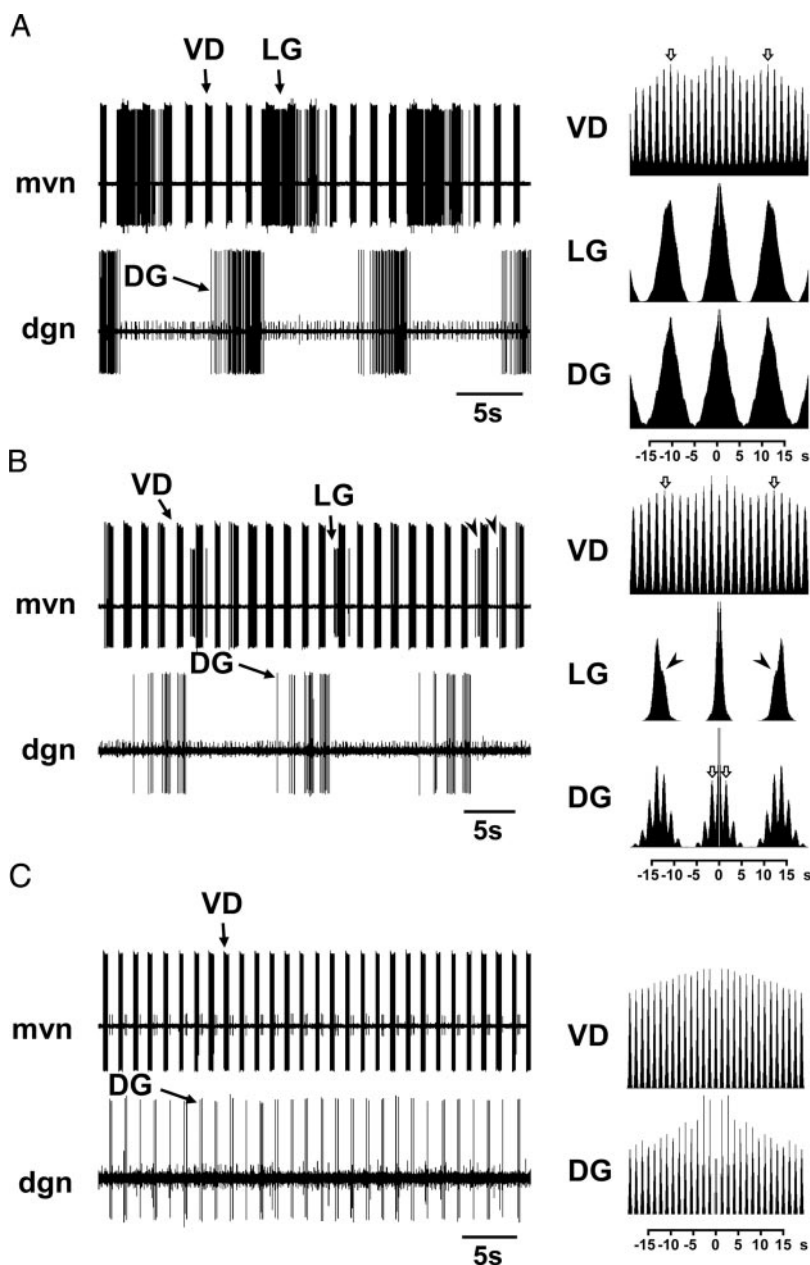
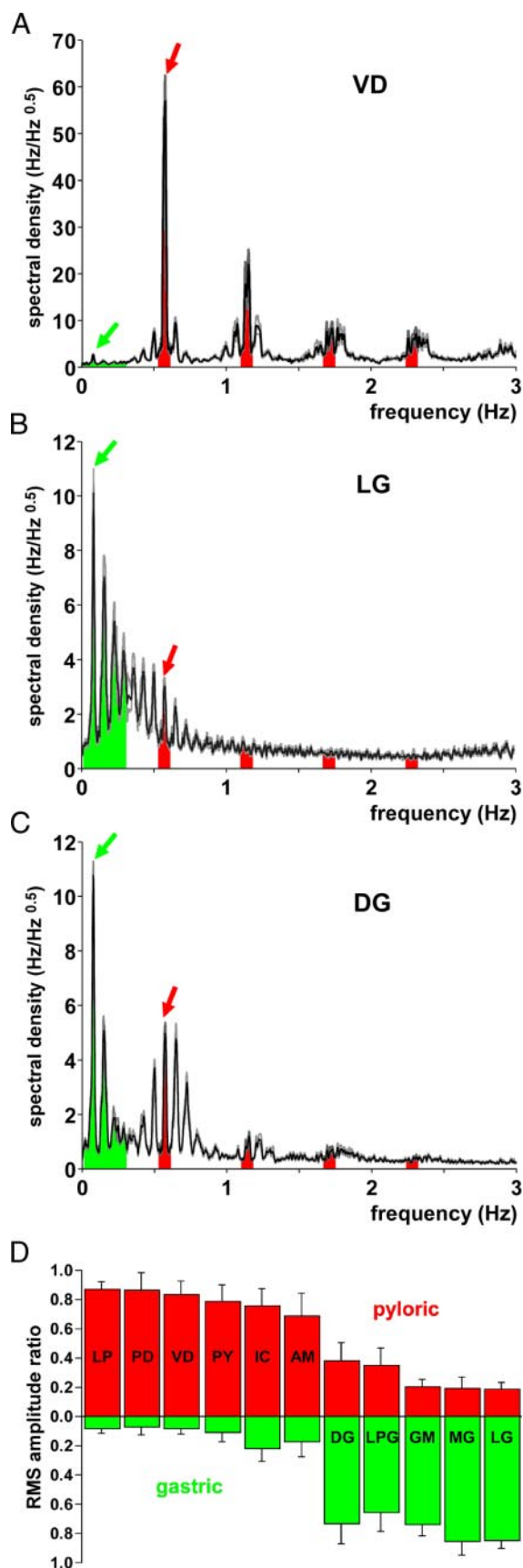


FIG. 12. Autocorrelations of STG neuron spike times. A—C, left: 3 example recordings of the mvn (VD and LG) and the dgn (DG). In C, no gastric rhythm was present, and the LG neuron was silent. Right: autocorrelations. The interval between every spike from a 20-min recording and every other spike in the same trace is plotted as a histogram around 0 (bin size: 50 ms). The VD neuron shows peaks corresponding to the pyloric cycle period (and its multiples) in all 3 examples. In A and B, these peaks are highest at the interval corresponding to the gastric cycle period (open arrows). The DG neuron shows peaks corresponding to the gastric cycle period in A, peaks corresponding to the gastric cycle period and multiples of the pyloric cycle period ( $\Downarrow$ ) in B, and only "pyloric peaks" in C. In B, the LG neuron showed pyloric modulation in cycles in which the duty cycle spanned  $>1$  pyloric cycle ( $\blacktriangledown$  in left panel). This pyloric modulation led to small shoulders at the peaks in the autocorrelation that correspond to the gastric cycle period (arrowheads in right panel).



neuron (open arrows). The LG neuron in this recording had a relatively small duty cycle that did not span multiple pyloric cycles in every gastric cycle. However, when it did, its firing pattern was clearly modulated in pyloric time (arrowheads in the mvn recording), which presumably results in the small shoulder of the gastric peak in the autocorrelation (arrowheads). The autocorrelations of the VD neuron and the DG neuron in Fig. 12C only show peaks corresponding to the pyloric cycle period.

#### Quantification of pyloric and gastric contribution to STG neuron firing patterns

On the qualitative level, the autocorrelations showed that the firing pattern of every STG neuron type can simultaneously contain timing information about both the fast pyloric rhythm and the slower gastric rhythm. However, we also wanted to establish the degree to which each rhythm contributes to the firing pattern of each individual neuron type.

To quantify the contribution of each rhythm to each cell's firing pattern, we examined the power spectrum of each cell's spike train (Fig. 13, A–C). We found that the spectra had most of their power in a series of sharp peaks, the first at the gastric mill frequency, and the others at integer multiples of this frequency. This is expected because any nonsinusoidal periodic signal with a given frequency can be written as a sum of sinusoids, the first at the given frequency, and the rest at integer multiples of the given frequency (Siebert 1986). The given frequency is often called the “fundamental,” and the other sinusoids are called “harmonics” of this fundamental. A purely gastric cell would be expected to have peaks at the gastric frequency (the fundamental) and integer multiples (harmonics) of the gastric frequency, and a purely pyloric cell would be expected to have peaks at the pyloric frequency and integer multiples of the pyloric frequency. Pyloric cells (VD in Fig. 13A) showed large peaks at the pyloric cycle frequency (red arrow) and integer multiples of it with the height of these pyloric-harmonic peaks decreasing steadily with increasing frequency. In addition, most pyloric cells also showed small peaks at the gastric frequency (green arrow), reflecting the pervasive gastric influences in the system. For gastric cells that had little or no apparent pyloric modulation of their firing pattern (LG in Fig. 13B), most of the power in the spectra were in peaks at the gastric frequency and harmonics of it, and the height of the harmonic peaks decreased steadily with increasing frequency. In cells that showed strong contributions of both rhythms (DG in Fig. 13C), we observed a blending of the purely pyloric and purely gastric spectra. In these cells, the height of the gastric harmonics did not decrease steadily with increasing frequency. Because of integer-locking of the gastric and pyloric frequencies, the pyloric frequency was a harmonic of the gastric frequency, and the peak at the pyloric fundamental tended to be much larger than it would have been in a purely gastric cell. The gastric harmonics just above and just below

FIG. 13. Spectral analysis of STG neuron spike activity. A–C: plots of spectral density vs. frequency for the VD, LG, and DG neuron recordings shown in Fig. 12B. The pyloric (red) and gastric (green) cycle frequencies are indicated by arrows. Shaded areas correspond to the frequency ranges used in the calculation of gastric and pyloric root-mean-square (RMS) amplitude ratios. D: gastric and pyloric RMS amplitude ratios for all STG neuron types ( $n = 10$ , AM:  $n = 5$ ).

the pyloric fundamental also tended to be enhanced. Above the pyloric fundamental, furthermore, the gastric harmonics that were not also pyloric harmonics tended to be very small or absent.

Based on these considerations, we felt justified in declaring all power below a particular cutoff (typically  $\sim 0.3$  Hz) to be gastric and all power in sharp peaks at the pyloric cycle frequency and multiples thereof to be pyloric. We quantified the gastric and pyloric contribution to the firing pattern of each neuron by integrating the power in the respective bands (red and green shading in Fig. 13, A–C) and then converting each to a root-mean-square (RMS) amplitude by taking the square root. These values were then normalized by dividing by the RMS amplitude in a wide band from 0 to 6 Hz. Although the gastric/pyloric ranges may not capture all of the gastric/pyloric power (e.g., Fig. 13B), they capture enough of it to be a useful quantification of the extent to which a cell's activity reflects gastric or pyloric activity.

Figure 13D shows the RMS amplitude ratios for the pyloric and gastric frequency ranges for every neuron type from 10 experiments. The AM neuron was only active in five of these experiments. Among the pyloric neurons, the gastric rhythm had the largest contribution to the firing pattern of the IC neuron. Among the gastric neurons, the pyloric rhythm had the largest contribution to the firing pattern of the DG neuron and the LPG neurons.

#### Firing pattern modulation by other rhythms

In five experiments, we recorded the esophageal rhythm, which is generated in the OG and CoGs and typically has a period somewhere in between the pyloric period and the gastric period ( $9.02 \pm 2.43$ ). We never observed clear firing pattern modulation of any of the pyloric and gastric neurons in time with that rhythm.

The cardiac sac rhythm, which has a cycle period on the order of tens of seconds to several minutes in the spiny lobster, has been shown to strongly influence pyloric firing patterns (Ayali and Harris-Warrick 1998; Moulins and Vedel 1977; Thuma and Hooper 2003). However, Meyrand et al. (1994) never saw spontaneous cardiac sac rhythms in *H. gammarus*. In one experiment, the gastric activity showed modulation with a period of tens of seconds, but we did not have a reference signal to determine if this was cardiac sac activity.

#### DISCUSSION

The simultaneous expression of more than one temporal pattern by neurons and networks is a widespread phenomenon. In the mammalian forebrain, oscillations are present in different frequency bands (Buzsaki and Chrobak 1995; Buzsaki and Draguhn 2004), and single neurons may express more than one type of oscillation at the same time (Steriade 2005; Steriade et al. 1993). In sensory systems, different firing modes can encode parallel and complementary information transfer (Oswald et al. 2004). In motor systems, interactions and coordination are particularly important, because many behaviors involve more than one body part (Chrachri and Neil 1993; Larson et al. 1994; Lieske et al. 2000; Morin and Viala 2002; Potts et al. 2005), and the coordinated execution of movements in neighboring body parts is important to avoid mechanical interference.

#### Quantification of circuit interactions

Although it may be commonplace for neurons to be driven by two or more rhythmic inputs, or even to be part of multiple rhythm-generating networks (Weimann and Marder 1994), quantification of the extent to which a neuron's firing reflects each of the rhythms is not easy, and one of our goals was to attempt this task using the pattern generating networks of the stomatogastric nervous system. We analyzed the interactions between the pyloric and the gastric rhythm in the lobster, *H. americanus*. Weimann et al. (1991) scored the STG neurons in *C. borealis* for the relative time they participate in either the gastric or the pyloric rhythm. This was relatively straightforward in a situation where neurons switch from one rhythm to the other (particularly when one of the rhythms is not always active) and when pyloric modulation during gastric bursts and gastric modulation of burst parameters in pyloric neurons is ignored. However, a quantification of the influence of one pattern on the activity of neurons that predominantly are critically involved in producing another pattern requires a different approach.

We analyzed the interactions between gastric and pyloric rhythms under different premises. A CPG can be viewed as a circuit, the constituent neurons of which produce a certain type of activity and are coordinated in a specific way. In the case of interactions with another circuit, the activity and the *intra*-circuit coordination may change within the reference frame of the other circuit's activity. We show here that the firing pattern produced by gastric neurons is influenced by the much faster pyloric rhythm. Some gastric neurons show pyloric-timed interruptions of their gastric-timed bursts, others show trailing firing in pyloric time between stronger gastric-timed bursts. We also show that the activity of the pyloric neurons, and their coordination within the pyloric pattern, change within the reference frame of the gastric cycle.

The presence of *inter*-circuit interactions is a separate issue from true coordination between the two patterns. In fact, spontaneous gastric and pyloric rhythms show no integer coupling in *P. interruptus* (Thuma and Hooper 2002). Nevertheless the overall spike frequency of pyloric neurons is strongly influenced by the gastric pattern. Thuma and Hooper (2002) show that using the gastric cycle as the frame of reference for a quantitative analysis in the absence of coordination leads to an underestimation of the magnitude of the interaction. This happens because of averaging between many gastric cycles in which pyloric cycles can occur at different times.

In *H. americanus*, the coordination between the two rhythms is stronger, as seen from the presence of integer coupling of the pyloric and gastric cycle periods. However, this coupling is variable, and 3 of 20 preparations failed to express it significantly. In addition, we show that all STG neurons express both patterns to some degree. Therefore there is no pure version of either of the two patterns that can serve as the reference frame for analyzing modulation of the other circuit.

In light of the preceding data, we also analyzed the spike patterns of each type of STG neuron independently. The goal was to quantify the contributions of each rhythm to the firing pattern. Integrating frequency bands of the power spectra that correspond to the cycle frequencies of the two rhythms provides a method that is independent of the presence of intercir-

cuit coordination. It also provides a means to collapse the influence of a pattern on the spiking activity of a given neuron into a single number, which is helpful for doing preparation-to-preparation comparisons and will be even more necessary for future quantifications of the extent to which neuromodulatory influences alter the interaction between the pyloric and gastric networks.

However, some caution is advisable when interpreting these numbers. For example, a neuron that fires in pyloric time, but only during a particular phase of the gastric cycle, will be "more pyloric" the longer its duty cycle in the gastric cycle according to our measure. Nevertheless the spectral analysis yielded results generally similar to what we found when we analyzed the pyloric firing patterns within the reference frame of the gastric rhythm, and the gastric firing pattern within the reference frame of the pyloric rhythm. Among the pyloric neurons, the gastric rhythm had the largest contribution to the firing pattern of the IC neuron. Among the gastric neurons, the pyloric rhythm had the largest contribution to the firing pattern of the DG neuron and the LPG neurons. The magnitude and functional relevance of these effects ultimately have to be seen in the context of the actual motor output (see following text).

#### *Is there a common baseline state of the isolated STNS from preparation to preparation?*

Under the influence of different neuromodulators and as a result of differential activation of descending modulatory neurons, the phase relationships of both the gastric pattern and the pyloric pattern can be very different (Dickinson and Nagy 1983; Eisen and Marder 1984; Flamm and Harris-Warrick 1986a,b; Heinzl 1988b; Heinzl and Selverston 1988; Marder and Hooper 1985; Marder and Weimann 1992; Marder et al. 2005; Meyrand et al. 2000; Nagy and Dickinson 1983; Norris et al. 1994; Nusbaum and Beenhakker 2002; Nusbaum et al. 2001). Nevertheless, the isolated STNS appears to have a comparable baseline activation state from preparation to preparation. In *H. americanus*, the pyloric cycle period can vary between 1.1 and 2.6 s from preparation to preparation, but the phase relationships are well conserved (Bucher et al. 2005).

Here we also found that the gastric rhythm was fairly consistent from preparation to preparation. To some degree, what constitutes a small or a large amount of variability lies in the eye of the beholder. Nonetheless, within the variability seen in every parameter we analyzed, we found gradual differences instead of distinct types of gastric activity or gastro-pyloric interactions. Distinct types of gastric activity or gastro-pyloric interactions are found in *C. borealis* when different modulatory projection neurons and/or sensory neurons are independently stimulated (Blitz et al. 2004; Norris et al. 1994; Nusbaum et al. 2001), but it is not known how consistent spontaneous activity of different modulatory projection neurons is.

In our data, the most extreme disparity appears to exist between the preparations that did not express spontaneous gastric activity and those that did. However, in the absence of gastric activity, the pyloric rhythm was slower (Fig. 3). Therefore it is possible that there is a continuum of how much overall descending modulatory activation of the two rhythms is present and that the threshold for activation of the gastric rhythm is higher than the one for the pyloric rhythm. This is not to say that modulatory input should be viewed as a general "arousal"

signal. It is now well established that activation and modulation of STG circuits is achieved through the activity of specific modulatory neurons and specific modulatory substances with specific cellular and synaptic targets (Blitz et al. 1995; Dickinson and Nagy 1983; Eisen and Marder 1984; Harris-Warrick et al. 1998; Nagy and Dickinson 1983; Nusbaum and Beenhakker 2002; Swensen and Marder 2000), and many modulatory neurons have target neurons in both the pyloric and gastric circuits (Blitz et al. 1999; Christie et al. 2004; Claiborne and Selverston 1984; Dickinson and Nagy 1983; Meyrand et al. 1991, 1994; Nagy et al. 1988; Nusbaum et al. 1992; Swensen and Marder 2000; Swensen et al. 2000). Nevertheless, only the pyloric rhythm sometimes persists even in the absence of modulatory inputs (Luther et al. 2003; Russell 1976; Weimann et al. 1997), and bath application of neuromodulators activates the gastric rhythm less readily than the pyloric rhythm (Heinzl and Selverston 1988; Marder et al. 1986).

#### *Functional implications of network interactions*

What do the interactions between gastric and pyloric activity mean with respect to the actual motor output? The ultimate decision about which part of the information present in a signal is functionally relevant is made at the readout, i.e., the postsynaptic site. For example, different types of synaptic dynamics can differentially filter frequency components of a presynaptic signal (Bertram 2001).

Accordingly, how much of the gastric and pyloric contributions to the firing pattern of a STG neuron is functionally relevant is decided at the structures postsynaptic to it. In *P. interruptus*, the overall spike frequency of pyloric neurons is modulated both through interactions with the gastric and the cardiac sac rhythms (Thuma and Hooper 2002, 2003). These changes, although subtle when considering predominant frequencies in the activity, can have large effects on the contraction amplitude of pyloric muscles (Morris et al. 2000; Thuma et al. 2003). This is a consequence of slow contraction and relaxation properties of the muscles that lead to low-pass filtering of the input (Hooper and Weaver 2000; Morris and Hooper 1998; Morris et al. 2000).

The contraction properties of stomach muscles in *H. americanus* have not been studied in detail. However, the gastric modulation of pyloric neuron firing may have similar effects on pyloric muscle contractions as in *P. interruptus*. Relatively slow relaxation time constants may lead to substantial amplitude changes over the gastric cycle. Possible effects of pyloric modulation of gastric neuron firing on gastric mill muscles are equally dependent on contraction properties. With very slow contraction/relaxation time constants, pyloric modulation of neurons innervating gastric mill muscles may result in little or no pyloric-timed contractions. With faster time constants, gastric mill muscles could contract in pyloric time on top of their gastric contractions or even produce "pure" pyloric contractions but confined to a specific phase of the gastric cycle.

Endoscopic imaging of the gastric mill in intact crabs has shown that the lateral teeth actually move in both gastric and pyloric time (Heinzl et al. 1993). It is also interesting to note that the contraction/relaxation time constants of gastric mill muscles in the crab can be changed substantially under the influence of different neurohormones (Jorge-Rivera et al. 1998). In principle, this means that the amount of pyloric-timed

contraction can be changed even if the pyloric contribution to the neuronal firing pattern stays the same.

Because the STG motor neurons are also part of the networks that generate the pyloric and gastric rhythms, they also have targets within the STG itself. As the synaptic connections within the STG show frequency-dependent synaptic depression (Manor et al. 1997; Nadim et al. 1999), and the membrane properties of STG neurons themselves may have slow dynamics (Goaillard and Marder 2005; Hooper 1998; Pulver et al. 2005), the extent to which the simultaneous expression of pyloric and gastric activity shapes the dynamics of circuit operation is at present hard to determine. It will be interesting in other systems that express two or more patterns simultaneously to determine the extent to which this is "seen" by their network targets.

#### ACKNOWLEDGMENTS

We thank C. Johnson for providing some of the data.

#### GRANTS

This work was supported by National Institute of Neurological Disorders and Stroke Grants NS-17813 to E. Marder and NS-050928 to A. L. Taylor.

#### REFERENCES

- Ayali A and Harris-Warrick RM.** Interaction of dopamine and cardiac sac modulatory inputs on the pyloric network in the lobster stomatogastric ganglion. *Brain Res* 794: 155–161, 1998.
- Bartos M, Manor Y, Nadim F, Marder E, and Nusbaum MP.** Coordination of fast and slow rhythmic neuronal circuits. *J Neurosci* 19: 6650–6660, 1999.
- Bartos M and Nusbaum MP.** Intercircuit control of motor pattern modulation by presynaptic inhibition. *J Neurosci* 17: 2247–2256, 1997.
- Bertram R.** Differential filtering of two presynaptic depression mechanisms. *Neural Comput* 13: 69–85, 2001.
- Blitz DM, Beenhakker MP, and Nusbaum MP.** Different sensory systems share projection neurons but elicit distinct motor patterns. *J Neurosci* 24: 11381–11390, 2004.
- Blitz DM, Christie AE, Coleman MJ, Norris BJ, Marder E, and Nusbaum MP.** Different proctolin neurons elicit distinct motor patterns from a multifunctional neuronal network. *J Neurosci* 19: 5449–5463, 1999.
- Blitz DM, Christie AE, Marder E, and Nusbaum MP.** Distribution and effects of tachykinin-like peptides in the stomatogastric nervous system of the crab, *Cancer borealis*. *J Comp Neurol* 354: 282–294, 1995.
- Bucher D, Prinz AA, and Marder E.** Animal-to-animal variability in motor pattern production in adults and during growth. *J Neurosci* 25: 1611–1619, 2005.
- Bucher D, Thirumalai V, and Marder E.** Axonal dopamine receptors activate peripheral spike initiation in a stomatogastric motor neuron. *J Neurosci* 23: 6866–6875, 2003.
- Buzsaki G and Chrobak JJ.** Temporal structure in spatially organized neuronal ensembles: a role for interneuronal networks. *Curr Opin Neurobiol* 5: 504–510, 1995.
- Buzsaki G and Draguhn A.** Neuronal oscillations in cortical networks. *Science* 304: 1926–1929, 2004.
- Chrachri A and Neil DM.** Interaction and synchronization between two abdominal motor systems in crayfish. *J Neurophysiol* 69: 1373–1383, 1993.
- Christie AE, Stein W, Quinlan JE, Beenhakker MP, Marder E, and Nusbaum MP.** Actions of a histaminergic/peptidergic projection neuron on rhythmic motor patterns in the stomatogastric nervous system of the crab *Cancer borealis*. *J Comp Neurol* 469: 153–169, 2004.
- Claiborne BJ and Ayers J.** Functional anatomy and behavior. In: *The Crustacean Stomatogastric System*, edited by Selverston AI and Moulins M. Berlin, Germany: Springer-Verlag, 1987, p. 9–29.
- Claiborne BJ and Selverston AI.** Histamine as a neurotransmitter in the stomatogastric nervous system of the spiny lobster. *J Neurosci* 4: 708–721, 1984.
- Clemens S, Combes D, Meyrand P, and Simmers J.** Long-term expression of two interacting motor pattern-generating networks in the stomatogastric system of freely behaving lobster. *J Neurophysiol* 79: 1396–1408, 1998.
- Dickinson PS.** Interactions among neural networks for behavior. *Curr Opin Neurobiol* 5: 792–798, 1995.
- Dickinson PS, Mecasas C, and Marder E.** Neuropeptide fusion of two motor-pattern generator circuits. *Nature* 344: 155–158, 1990.
- Dickinson PS and Nagy F.** Control of a central pattern generator by an identified modulatory interneuron in *Crustacea*. II. Induction and modification of plateau properties in pyloric neurons. *J Exp Biol* 105: 59–82, 1983.
- Eisen JS and Marder E.** A mechanism for production of phase shifts in a pattern generator. *J Neurophysiol* 51: 1375–1393, 1984.
- Faumont S, Simmers J, and Meyrand P.** Activation of a lobster motor rhythm-generating network by disinhibition of permissive modulatory inputs. *J Neurophysiol* 80: 2776–2780, 1998.
- Flamm RE and Harris-Warrick RM.** Aminergic modulation in lobster stomatogastric ganglion. I. Effects on motor pattern and activity of neurons within the pyloric circuit. *J Neurophysiol* 55: 847–865, 1986a.
- Flamm RE and Harris-Warrick RM.** Aminergic modulation in lobster stomatogastric ganglion. II. Target neurons of dopamine, octopamine, and serotonin within the pyloric circuit. *J Neurophysiol* 55: 866–881, 1986b.
- Friedrich RW, Habermann CJ, and Laurent G.** Multiplexing using synchrony in the zebrafish olfactory bulb. *Nat Neurosci* 7: 862–871, 2004.
- Goaillard JM and Marder E.** Short-term dynamics of potassium conductances in a crustacean motor neuron. *Soc Neurosci Abstr* 177.22, 2005.
- Harris-Warrick RM, Johnson BR, Peck JH, Kloppenburg P, Ayali A, and Skarbinski J.** Distributed effects of dopamine modulation in the crustacean pyloric network. *Ann NY Acad Sci* 860: 155–167, 1998.
- Harris-Warrick R, Marder E, Selverston AI, and Moulins M.** *Dynamic Biological Networks: The Stomatogastric Nervous System*. Cambridge, MA: MIT Press, 1992.
- Heinzel HG.** Gastric mill activity in the lobster. I. Spontaneous modes of chewing. *J Neurophysiol* 59: 528–550, 1988a.
- Heinzel HG.** Gastric mill activity in the lobster. II. Proctolin and octopamine initiate and modulate chewing. *J Neurophysiol* 59: 551–565, 1988b.
- Heinzel HG and Selverston AI.** Gastric mill activity in the lobster. III. Effects of proctolin on the isolated central pattern generator. *J Neurophysiol* 59: 566–585, 1988.
- Heinzel HG, Weimann JM, and Marder E.** The behavioral repertoire of the gastric mill in the crab, *Cancer pagurus*: an in situ endoscopic and electrophysiological examination. *J Neurosci* 13: 1793–1803, 1993.
- Hooper SL.** Transduction of temporal patterns by single neurons. *Nat Neurosci* 1: 720–726, 1998.
- Hooper SL and Moulins M.** Switching of a neuron from one network to another by sensory-induced changes in membrane properties. *Science* 244: 1587–1589, 1989.
- Hooper SL and Moulins M.** Cellular and synaptic mechanisms responsible for a long-lasting restructuring of the lobster pyloric network. *J Neurophysiol* 64: 1574–1589, 1990.
- Hooper SL and Weaver AL.** Motor neuron activity is often insufficient to predict motor response. *Curr Opin Neurobiol* 10: 676–682, 2000.
- Jorge-Rivera JC, Sen K, Birmingham JT, Abbott LF, and Marder E.** Temporal dynamics of convergent modulation at a crustacean neuromuscular junction. *J Neurophysiol* 80: 2559–2570, 1998.
- Larson CR, Yajima Y, and Ko P.** Modification in activity of medullary respiratory-related neurons for vocalization and swallowing. *J Neurophysiol* 71: 2294–2304, 1994.
- Lieske SP, Thoby-Brisson M, Telgkamp P, and Ramirez JM.** Reconfiguration of the neural network controlling multiple breathing patterns: eupnea, sighs, and gasps. *Nat Neurosci* 3: 600–607, 2000.
- Luther JA, Robie AA, Yarotsky J, Reina C, Marder E, and Golowasch J.** Episodic bouts of activity accompany recovery of rhythmic output by a neuromodulator- and activity-deprived adult neural network. *J Neurophysiol* 90: 2720–2730, 2003.
- Manor Y, Nadim F, Abbott LF, and Marder E.** Temporal dynamics of graded synaptic transmission in the lobster stomatogastric ganglion. *J Neurosci* 17: 5610–5621, 1997.
- Marder E, Bucher D, Schulz DJ, and Taylor AL.** Invertebrate central pattern generation moves along. *Curr Biol* 15: R685–699, 2005.
- Marder E and Hooper SL.** Neurotransmitter modulation of the stomatogastric ganglion of decapod crustaceans. In: *Model Neural Networks and Behavior*, edited by Selverston AI. New York: Plenum, 1985, p. 319–337.
- Marder E, Hooper SL, and Siwicki KK.** Modulatory action and distribution of the neuropeptide proctolin in the crustacean stomatogastric nervous system. *J Comp Neurol* 243: 454–467, 1986.
- Marder E and Weimann JM.** Modulatory control of multiple task processing in the stomatogastric nervous system. In: *Neurobiology of Motor Programme*

- Selection*, edited by Kien J, McCrohan C, and Winlow B. New York: Pergamon, 1992, p. 3–19.
- Maynard DM and Dando MR.** The structure of the stomatogastric neuromuscular system in *Callinectes sapidus*, *Homarus americanus*, and *Panulirus argus* (Decapoda Crustacea). *Philos Trans R Soc Lond B* 268: 161–220, 1974.
- Meyrand P, Faumont S, Simmers J, Christie AE, and Nusbaum MP.** Species-specific modulation of pattern-generating circuits. *Eur J Neurosci* 12: 2585–2596, 2000.
- Meyrand P, Simmers J, and Moulins M.** Construction of a pattern-generating circuit with neurons of different networks. *Nature* 351: 60–63, 1991.
- Meyrand P, Simmers J, and Moulins M.** Dynamic construction of a neural network from multiple pattern generators in the lobster stomatogastric nervous system. *J Neurosci* 14: 630–644, 1994.
- Miller WL and Sigvardt KA.** Spectral analysis of oscillatory neural circuits. *J Neurosci Methods* 80: 113–128, 1998.
- Morin D and Viala D.** Coordinations of locomotor and respiratory rhythms in vitro are critically dependent on hindlimb sensory inputs. *J Neurosci* 22: 4756–4765, 2002.
- Morris LG and Hooper SL.** Muscle response to changing neuronal input in the lobster (*Panulirus interruptus*) stomatogastric system: slow muscle properties can transform rhythmic input into tonic output. *J Neurosci* 18: 3433–3442, 1998.
- Morris LG, Thuma JB, and Hooper SL.** Muscles express motor patterns of non-innervating neural networks by filtering broad-band input. *Nat Neurosci* 3: 245–250, 2000.
- Moulins M and Vedel JP.** Central organization of rhythmic motor activity of the foregut in decapoda Crustacea. *J Physiol* 73: 471–510, 1977.
- Mulloney B.** Organization of the stomatogastric ganglion of the spiny lobster. V. Coordination of the gastric and pyloric systems. *J Comp Physiol* 122: 227–240, 1977.
- Mulloney B.** Neural circuits. In: *The Crustacean Stomatogastric System*, edited by Selverston AI and Moulins M. Berlin, Germany: Springer, 1987 p. 57–75.
- Mulloney B and Selverston AI.** Organization of the stomatogastric system in the spiny lobster. III. Coordination of the two subsets of the gastric system. *J Comp Physiol* 91: 53–78, 1974.
- Nadim F, Manor Y, Kopell N, and Marder E.** Synaptic depression creates a switch that controls the frequency of an oscillatory circuit. *Proc Natl Acad Sci USA* 96: 8206–8211, 1999.
- Nadim F, Manor Y, Nusbaum MP, and Marder E.** Frequency regulation of a slow rhythm by a fast periodic input. *J Neurosci* 18: 5053–5067, 1998.
- Nagy F, Cardi P, and Cournil I.** A rhythmic modulatory gating system in the stomatogastric nervous system of *Homarus gammarus*. I. Pyloric-related neurons in the commissural ganglia. *J Neurophysiol* 71: 2477–2489, 1994.
- Nagy F and Dickinson PS.** Control of a central pattern generator by an identified modulatory interneuron in *Crustacea*. I. Modulation of the pyloric motor output. *J Exp Biol* 105: 33–58, 1983.
- Nagy F, Dickinson PS, and Moulins M.** Control by an identified modulatory neuron of the sequential expression of plateau properties of, and synaptic inputs to, a neuron in a central pattern generator. *J Neurosci* 8: 2875–2886, 1988.
- Norris BJ, Coleman MJ, and Nusbaum MP.** Recruitment of a projection neuron determines gastric mill motor pattern selection in the stomatogastric nervous system of the crab, *Cancer borealis*. *J Neurophysiol* 72: 1451–1463, 1994.
- Nusbaum MP and Beenhakker MP.** A small-systems approach to motor pattern generation. *Nature* 417: 343–350, 2002.
- Nusbaum MP, Blitz DM, Swensen AM, Wood D, and Marder E.** The roles of co-transmission in neural network modulation. *Trends Neurosci* 24: 146–154, 2001.
- Nusbaum MP, Weimann JM, Golowasch J, and Marder E.** Presynaptic control of modulatory fibers by their neural network targets. *J Neurosci* 12: 2706–2714, 1992.
- Oswald AM, Chacron MJ, Doiron B, Bastian J, and Maler L.** Parallel processing of sensory input by bursts and isolated spikes. *J Neurosci* 24: 4351–4362, 2004.
- Percival DB and Walden AT.** *Spectral Analysis for Physical Applications, Multitaper and Conventional Univariate Techniques*. Cambridge, New York: Cambridge, 1993.
- Potts JT, Rybak IA, and Paton JF.** Respiratory rhythm entrainment by somatic afferent stimulation. *J Neurosci* 25: 1965–1978, 2005.
- Pulver SR, Taylor AL, and Marder E.** Multi-cycle adaptation to rhythmic synaptic drive. *Soc Neurosci Abstr* 177.23, 2005.
- Robertson RM and Moulins M.** Oscillatory command input to the motor pattern generators of the crustacean stomatogastric ganglion. II. The gastric rhythm. *J Comp Physiol [A]* 154: 473–491, 1984.
- Russell DF.** Rhythmic excitatory inputs to the lobster stomatogastric ganglion. *Brain Res* 101: 582–588, 1976.
- Selverston AI and Miller JP.** Mechanisms underlying pattern generation in lobster stomatogastric ganglion as determined by selective inactivation of identified neurons. I. Pyloric system. *J Neurophysiol* 44: 1102–1121, 1980.
- Selverston AI and Moulins M.** *The Crustacean Stomatogastric System*. Berlin, Germany: Springer, 1987.
- Selverston AI, Russell DF, Miller JP, and King DG.** The stomatogastric nervous system: structure and function of a small neural network. *Prog Neurobiol* 7: 215–290, 1976.
- Siebert WM.** *Circuits, Signals, and Systems*. Cambridge, MA: MIT Press, 1986.
- Steriade M.** Grouping of brain rhythms in corticothalamic systems. *Neuroscience* 137: 1087–1106, 2006.
- Steriade M, Nunez A, and Amzica F.** Intracellular analysis of relations between the slow (< 1 Hz) neocortical oscillation and other sleep rhythms of the electroencephalogram. *J Neurosci* 13: 3266–3283, 1993.
- Swensen AM, Golowasch J, Christie AE, Coleman MJ, Nusbaum MP, and Marder E.** GABA and responses to GABA in the stomatogastric ganglion of the crab *Cancer borealis*. *J Exp Biol* 203: 2075–2092, 2000.
- Swensen AM and Marder E.** Multiple peptides converge to activate the same voltage-dependent current in a central pattern-generating circuit. *J Neurosci* 20: 6752–6759, 2000.
- Thirumalai V and Marder E.** Colocalized neuropeptides activate a central pattern generator by acting on different circuit targets. *J Neurosci* 22: 1874–1882, 2002.
- Thomson DJ and Chave AD.** Jackknifed error estimates for spectra, coherences, and transfer functions. In: *Advances in Spectral Analysis and Array Processing*, edited by Haykin S. Englewood Cliffs, NJ: Prentice-Hall, 1991, p. 58–113.
- Thuma JB and Hooper SL.** Quantification of gastric mill network effects on a movement related parameter of pyloric network output in the lobster. *J Neurophysiol* 87: 2372–2384, 2002.
- Thuma JB and Hooper SL.** Quantification of cardiac sac network effects on a movement-related parameter of pyloric network output in the lobster. *J Neurophysiol* 89: 745–753, 2003.
- Thuma JB, Morris LG, Weaver AL, and Hooper SL.** Lobster (*Panulirus interruptus*) pyloric muscles express the motor patterns of three neural networks, only one of which innervates the muscles. *J Neurosci* 23: 8911–8920, 2003.
- Weimann JM and Marder E.** Switching neurons are integral members of multiple oscillatory networks. *Curr Biol* 4: 896–902, 1994.
- Weimann JM, Marder E, Evans B, and Calabrese RL.** The effects of SDRNFLRFamide and TNRNFLRFamide on the motor patterns of the stomatogastric ganglion of the crab *Cancer borealis*. *J Exp Biol* 181: 1–26, 1993.
- Weimann JM, Meyrand P, and Marder E.** Neurons that form multiple pattern generators: identification and multiple activity patterns of gastric/pyloric neurons in the crab stomatogastric system. *J Neurophysiol* 65: 111–122, 1991.
- Weimann JM, Skiebe P, Heinzel HG, Soto C, Kopell N, Jorge-Rivera JC, and Marder E.** Modulation of oscillator interactions in the crab stomatogastric ganglion by crustacean cardioactive peptide. *J Neurosci* 17: 1748–1760, 1997.
- Wood DE, Manor Y, Nadim F, and Nusbaum MP.** Intercircuit control via rhythmic regulation of projection neuron activity. *J Neurosci* 24: 7455–7463, 2004.